DOI: 10.1002/ejoc.200900983

Dye-Sensitized Solar Cells Based on a Novel Fluorescent Dye with a Pyridine Ring and a Pyridinium Dye with the Pyridinium Ring Forming Strong Interactions with Nanocrystalline TiO_2 Films

Yousuke Ooyama,[a] Shogo Inoue,[a] Risa Asada,[a] Genta Ito,[a] Kohei Kushimoto,[a] Kenji Komaguchi,[a] Ichiro Imae,[a] and Yutaka Harima*[a]

Keywords: Solar cells / Titanium / Sensitizers / Dyes/pigments / Fluorescence

As new-type donor–acceptor π-conjugated dyes capable of forming a strong interaction between the electron-acceptor moiety of the sensitizers and a TiO_2 surface, fluorescent dye **OH11** and pyridinum dye **OH12** with a pyridine and pyridinium ring as the electron-accepting group, respectively, have been designed and synthesized as photosensitizers for use in dye-sensitized solar cells (DSSCs). The fluorescent dye **OH11** exhibits an absorption band at around 410 nm and a fluorescence band at around 530 nm. On the other hand, the pyridinum dye **OH12** shows an absorption maximum at around 560 nm, assigned to a strong intramolecular charge-transfer excitation from the dibutylamino group to the pyridinium ring. The short-circuit photocurrent densities of the DSSCs prepared by using **OH11** and **OH12** are 4.33 and 1.74 mA cm^{-2}, and the solar energy-to-electricity conversion yields are 1.33 and 0.51 %, respectively, under simulated solar light [AM (air mass) 1.5, 100 mW cm^{-2}]. The open-circuit photovoltage for **OH11** (525 mV) is higher than that of **OH12** (444 mV). The effects of the configuration of the dyes on the TiO_2 surface and of their chemical structures on the photovoltaic performances are discussed on the basis of semi-empirical molecular orbital calculations (AM1 and INDO/S), spectral analyses and cyclic voltammetry.

Introduction

Dye-sensitized solar cells (DSSCs) based on dye sensitizers adsorbed on nanocrystalline TiO_2 electrodes have received considerable attention because of high-incident solar light-to-electricity conversion efficiency, colourful and decorative cells, and the low cost of production.[1,2] A large variety of organic dyes have been developed, and the relationship between the chemical structures and photovoltaic performances of the DSSCs has been examined.[3–12] Among them, donor–acceptor π-conjugated (D–π–A) dyes with both electron-donating (D) and -accepting (A) groups linked by a π-conjugated bridge possessing broad and intense absorption spectral features are expected to be amongst the most promising organic sensitizers.[3–8] Most of the D–π–A dyes have dialkylamine or diphenylamine moieties as the electron donor and a carboxylic, cyanoacrylic or rhodanine-3-acetic acid moiety acting as the electron acceptor as well as the anchoring group for attachment to the TiO_2 surface. The carboxy group can form an ester linkage with the TiO_2 surface to provide a strongly bound dye and good electron communication between them. However, the development of new donor–acceptor π-conjugated dyes for DSSCs is limited because a carboxy group is necessary in combination with a π-conjugated system or electron-accepting moiety for the above reasons. To create new and efficient D–π–A dyes for DSSCs, epoch-making molecular design, such as the formation of a strong interaction between the electron-accepting moiety of sensitizers and the TiO_2 surface, is required.

Recently, as D–π–A dye sensitizers to meet the above requirements, we designed and synthesized a series of novel benzofuro[2,3-*c*]oxazolo[4,5-*a*]carbazole-type fluorescent dyes **OH1**–**4** with carboxy groups at different positions of a chromophore skeleton (Scheme 1).[13] In dye **OH1**, the carboxy group acts not only as the anchoring group for attachment to the TiO_2 surface but also as the electron acceptor. For **OH2**, **OH3** and **OH4**, on the other hand, the carboxy group acts as the anchoring group; however, the electron acceptor is not a carboxy group but a cyano group. The photovoltaic performance of **OH2**, which has a non-conjugated linkage between the carboxy group and the chromophore, is similar to that of **OH1** and higher than those of **OH3** and **OH4**. In **OH1**, electrons can be injected efficiently from the carboxy group to the conduction band of a TiO_2 electrode through the ester linkage formed with the TiO_2 surface. On the other hand, in the molecular structure of **OH2**, it was suggested that the phenylcyano group,

[a] Department of Applied Chemistry, Graduate School of Engineering, Hiroshima University,
Higashi-Hiroshima 739-8527, Japan
Fax: +81-82-424-5494
E-mail: harima@mls.ias.hiroshima-u.ac.jp

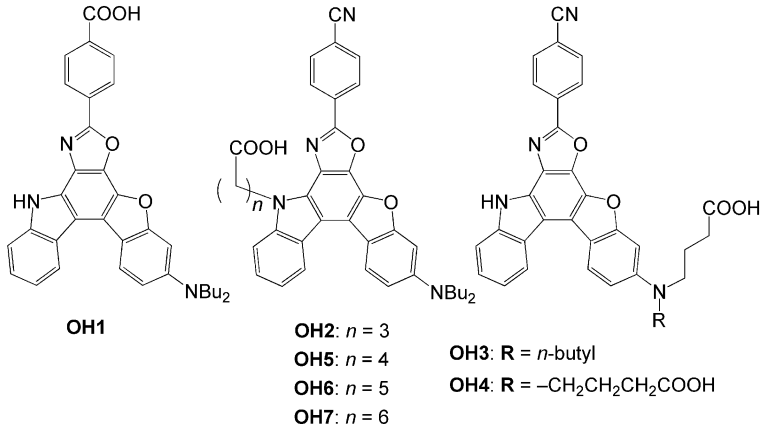

Scheme 1. Molecular structures of benzofuro[2,3-*c*]oxazolo[4,5-*a*]carbazole-type fluorescent dye sensitizers **OH1**–**7**.

acting as an electron acceptor, is located in close proximity to the TiO_2 surface through an interaction such as an intermolecular hydrogen bond between the cyano nitrogen atom of the dye and a hydroxy proton at the TiO_2 surface. Consequently, dye **OH2** can efficiently inject electrons from the phenylcyano group into the conduction band of a TiO_2 electrode through intermolecular hydrogen bonding. To provide further confirmation of this, dyes **OH5**–**7**, with different lengths of non-conjugated alkyl chains with a terminal carboxy group, have been designed and synthesized (Scheme 1).[14] It was found that in spite of the lengths of the alkyl chains, due to the flexibility of the alkyl chain, the cyano group of the dyes is located close to the TiO_2 surface, and thus good electron communication between the dyes and the TiO_2 surface is established. Thus, it was concluded that the carboxy group of a donor–acceptor π-conjugated sensitizer is necessary not as an electron acceptor, but only as an anchoring group for attachment to the TiO_2 surface. This implies that the crucial criterion for developing new and efficient donor–acceptor π-conjugated sensitizers for DSSCs is the ability of the sensitizer molecule to form a strong interaction between the electron-acceptor moiety of the sensitizer and the TiO_2 surface.

In this study, as new-type D–π–A dye sensitizers capable of forming a strong interaction between the electron-acceptor moiety of the sensitizers and the TiO_2 surface, a novel fluorescent dye **OH11** and a pyridinium dye **OH12** with a pyridine and pyridinium ring, respectively, as the electron-accepting group, have been designed and synthesized (Scheme 2). These dyes have a non-conjugated alkyl chain with a terminal carboxy group such that the carboxy anchoring group is separated from the electron-acceptor moiety. It is well known that pyridine is adsorbed on the TiO_2 surface through the formation of a hydrogen bond between the nitrogen of the pyridine and a hydroxy proton at the TiO_2 surface.[15,16] On the other hand, the cationic pyridinium moiety is adsorbed on the TiO_2 surface through the formation of a strong electrostatic interaction between the cationic pyridinium ring and an anionic site, such as a hydroxy group at the TiO_2 surface and an oxygen atom in TiO_2. Therefore, we expect that the pyridine and pyridinium rings of **OH11** and **OH12** are located close to the TiO_2 surface, and thus good electron communication is established between the dyes and the TiO_2 surface. With this in mind, the photovoltaic performances of DSSCs based on **OH11** with a pyridine ring and **OH12** with a pyridinium ring were measured. In addition, we synthesized a new fluorescent dye **OH13** with 2,2′-bipyridin-4-carboxylic acid as the electron-accepting group; the carboxy group of **OH13** is not conjugated to the electron-donating dibutylamino group. The effects of the configurations of **OH11**, **OH12** and **OH13** at the TiO_2 surface and of their chemical structures on the photovoltaic performance are discussed on the basis of semi-empirical molecular orbital calculations (AM1 and INDO/S), spectral analyses and cyclic voltammetry (CV).

Results and Discussion

Synthesis of D–π–A Dye Sensitizers OH11, OH12 and OH13

The synthetic pathway to D–π–A dye sensitizers **OH11**, **OH12** and **OH13** is shown in Scheme 2. We used 3-dibutylamino-8*H*-5-oxa-8-azaindeno[2,1-*c*]fluorene-6,7-dione (**1**)[13,14] as the starting material. The quinone **1** was allowed to react with 4-pyridinecarbaldehyde in the presence of an excess of ammonium acetate in acetic acid to give the structural isomers **2** and **3** in 31 and 12% yields, respectively. The reaction of **2** with ethyl 4-bromobutyrate by using sodium hydride yielded **4**. The fluorescent dye **OH11** was obtained in 94% yield by hydrolysis of **4**. The reaction of **OH11** with 1-iodobutane gave the pyridinium dye **OH12** in 62% yield. On the other hand, the fluorescent dye **OH13** was synthesized in 33% yield by the reaction of 2,2′-bipyridin-4,4′-dicarbaldehyde with the quinone **1** in the presence of an excess of ammonium acetate in acetic acid. In this reaction, an aldehyde was oxidized to the carboxy group.

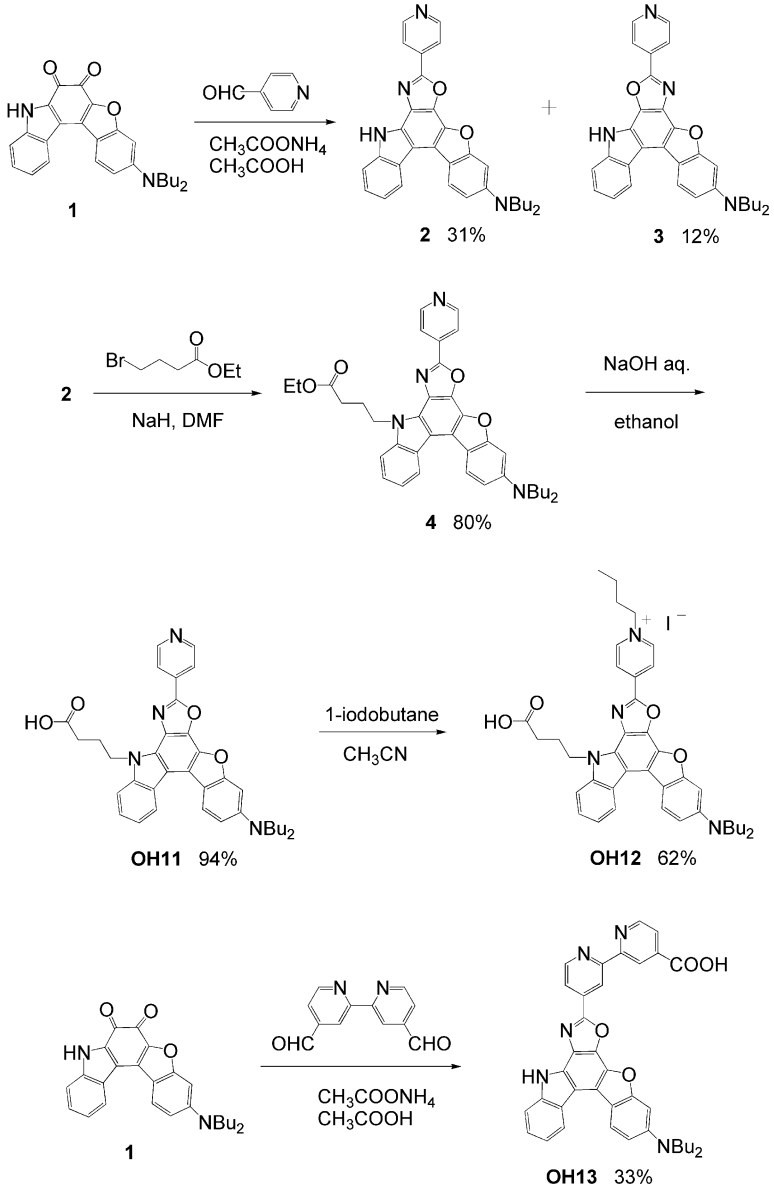

Scheme 2. Synthesis of **OH11**, **OH12** and **OH13**.

Spectroscopic Properties of OH11, OH12 and OH13 in Solution and Adsorbed on TiO_2 Film

The visible absorption and fluorescence spectroscopic data of **OH11**, **OH12** and **OH13** in THF are summarized in Table 1, and the spectra are shown in Figure 1. The three dyes show two absorption maxima: one band occurs at 350–370 nm, ascribed to a $\pi \rightarrow \pi^*$ transition, and another band at 410–425 or 560 nm, assigned to intramolecular charge transfer (ICT) excitation from the dibutylamino group to the pyridine ring for **OH11** and **OH13** or to the pyridinium ring for **OH12**. The ICT band of **OH12** occurs at a longer wavelength than those of **OH11** and **OH13**. The corresponding fluorescence bands for **OH11** and **OH13** are observed at around 533 and 559 nm, respectively. The fluorescence quantum yield of **OH11** (Φ = 0.86) is higher than that of **OH13** (Φ = 0.34), whereas the pyridinium dye **OH12** does not exhibit any observable fluorescence.

Table 1. Spectroscopic properties of **OH11**, **OH12** and **OH13** in THF.

Dye	λ_{max}^{abs} [nm] (ε_{max} [$dm^3 mol^{-1} cm^{-1}$])	λ_{max}^{fl} [nm]	Φ[a]	SS[b] [nm]
OH11	349 (31000), 412 (26600)	533	0.86	121
OH12	368 (43000), 560 (12200)	–	–	–
OH13	351 (36000), 425 (23700)	559	0.34	134

[a] The Φ values were determined by using a calibrated integrating sphere system (λ_{ex} = 325 nm). [b] Stokes shift value.

The absorption spectra of the dyes adsorbed on the TiO_2 film are shown in Figure 2. The absorption peak wavelengths are redshifted by 38 nm for **OH11**, 22 nm for **OH12**

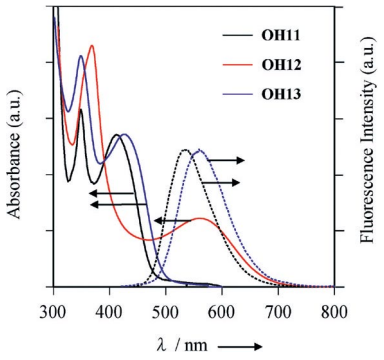

Figure 1. Absorption (–) and fluorescence (···) spectra of **OH11**, **OH12** and **OH13** in THF.

and 20 nm for **OH13** relative to those in THF. The large redshift for **OH11** may be due to the formation of a hydrogen bond between the nitrogen atom of the pyridine ring and the hydroxy proton at the TiO_2 surface. Moreover, the onsets of the absorption bands are redshifted by 80–120 nm, which is attributable to dye aggregation at the TiO_2 electrode.[8,13]

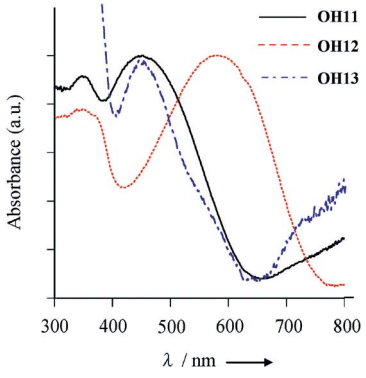

Figure 2. Absorption spectra of **OH11**, **OH12** and **OH13** adsorbed on TiO_2 film.

Electrochemical Properties of OH11, OH12 and OH13 and Their HOMO and LUMO Energy Levels

The electrochemical properties of the three dyes were determined by cyclic voltammetry (CV) in DMF containing 0.1 M Et_4NClO_4. As an example, the CV curve of **OH11** is shown in Figure 3. The CV data are summarized in Table 2. The oxidation peaks for **OH11**, **OH12** and **OH13** were observed at 0.40, 0.40 and 0.35 V versus Ag/Ag^+, respectively. The corresponding reduction peaks for **OH11** and **OH13** appeared at 0.35 and 0.25 V, respectively, whereas no reduction peak was observed for **OH12**. These results show that the oxidized states of the dyes, with the exception of **OH12**, are stable.

The HOMO and LUMO energy levels of these dyes were evaluated from the spectral and CV data. The HOMO energy levels for **OH11**, **OH12** and **OH13** were determined to be 0.96, 0.96 and 0.91 V with respect to a normal hydrogen electrode (NHE), respectively. The LUMO energy levels of

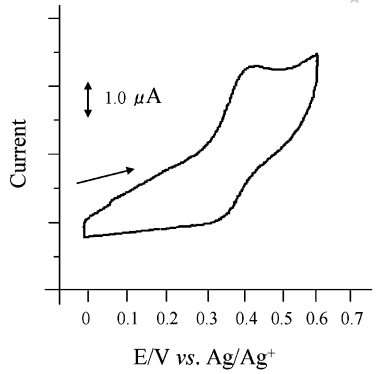

Figure 3. Cyclic voltammogram of **OH11** in DMF containing 0.1 M Et_4NClO_4 at a scan rate of 50 mV s^{-1}. The arrow denotes the direction of the potential scan.

Table 2. Electrochemical properties of **OH11**, **OH12** and **OH13** and their HOMO and LUMO energy levels.

Dye	E_{pa}[a] [V]	E_{pc}[b] [V]	HOMO[c] [V]	LUMO[c] [V]
OH11	0.40	0.35	0.96	–1.62
OH12	0.40	–	0.96	–0.81
OH13	0.35	0.25	0.91	–1.62

[a] E_{pa} is the anodic peak potential vs. Ag/Ag^+ in acetonitrile. [b] E_{pc} is the cathodic peak potential vs. Ag/Ag^+ in acetonitrile. [c] Vs. a normal hydrogen electrode (NHE).

OH11 and **OH13** were estimated from the oxidation potentials and the intersection of the absorption and fluorescence spectra [480 nm (2.58 eV) for **OH11** and 490 nm (2.53 eV) for **OH13**], which corresponds to the energy gap between the HOMO and the LUMO. The LUMO energy levels of **OH11** and **OH13** are both –1.62 V. On the other hand, the LUMO energy level of **OH12**, which was estimated from the oxidation potential and the onset of the absorption band [700 nm (1.77 eV)], is –0.81 V, which shows that substitution of the pyridine ring to give the pyridinium ring lowers the LUMO level considerably. The LUMO energy levels of **OH11** and **OH13** are higher than that of the TiO_2 conduction band (–0.5 V), which suggests that efficient electron injection into the TiO_2 conduction band is thermodynamically possible. The LUMO levels of **OH11** and **OH13** are more negative than that of **OH12**, which indicates that the dyes **OH11** and **OH13** have more efficient electron-injection ability than **OH12**.

Semi-Empirical MO Calculations (AM1 and INDO/S) on OH11, OH12 and OH13

The photophysical and electrochemical properties of **OH11**, **OH12** and **OH13** were analysed by semi-empirical molecular orbital (MO) calculations. The molecular structures were optimized by the MOPAC/AM1 method,[17] and then the INDO/S method[18] using the SCRF Onsager model was used for spectroscopic calculations in THF. The calculated absorption wavelengths and the transition char-

acters of the first absorption bands are collected in Table 3. The calculated absorption wavelengths and the oscillator strengths *f* for **OH11**, **OH12** and **OH13** are comparable to the observed spectra in THF: the calculated absorption wavelength of **OH12** is shifted to a longer wavelength than those of **OH11** and **OH13**, which is in good agreement with the experimental data in THF. The calculations show that the longest excitation bands of 420 nm for **OH11** and **OH13** and 544 nm for **OH12** can mainly be assigned to the transition from the HOMO to the LUMO for **OH11** and **OH13** and from the HOMO to the NLUMO for **OH13**, with the HOMOs mostly localized on the 3-(dibutylamino)-benzofuro[2,3-*c*]oxazolo[4,5-*a*]carbazole moiety for the three dyes and the LUMOs and NLUMO mostly localized on the pyridine ring for **OH11**, the bipyridine ring for **OH13** and the pyridinium ring for **OH12**, respectively. The changes in the calculated electron density accompanying the first electron excitation are shown in Figure 4, which reveals a strong migration of the intramolecular charge transfer (ICT) from the 3-(dibutylamino)benzofuro[2,3-*c*]-oxazolo[4,5-*a*]carbazole moiety to the pyridine, bipyridine or pyridinium rings for the three dyes. The calculations have revealed that the ICT of **OH12** is stronger than those of **OH11** and **OH13**, which accounts for the large redshift of the ICT band for **OH12**.

Table 3. Calculated absorption spectra for **OH11**, **OH12** and **OH13**.

Dye	μ[a] [D]	Absorption (calcd.) λ_{max} [nm]	f[b]	CI component[c]	$\Delta\mu$[d] [D]
OH11	9.50	420	0.74	HOMO→LUMO (79%)	12.76
OH12	21.29	544	0.85	HOMO→LUMO (83%)	19.51
OH13	5.41	420	0.79	HOMO→LUMO (20%) HOMO→NLUMO (59%)	12.73

[a] Dipole moment in the ground state. [b] Oscillator strength. [c] The transition is shown by an arrow from one orbital to another, followed by its percentage CI (configuration interaction) component. [d] Difference in the dipole moment between the excited and ground states.

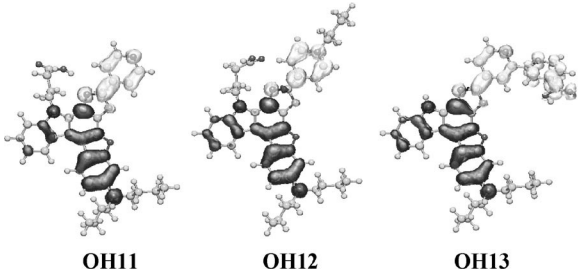

Figure 4. Calculated electron-density changes accompanying the first electronic excitation of **OH11**, **OH12** and **OH13**. The black and white lobes, respectively, signify the decrease and increase in the electron density accompanying the electronic transition. Their areas indicate the magnitude of the electron-density change.

Photovoltaic Performances of DSSCs Based on OH11, OH12 and OH13

The DSSCs were fabricated by using a dye-adsorbed TiO_2 electrode, Pt-coated glass as the counter electrode and an acetonitrile solution containing 0.05 M iodine, 0.1 M lithium iodide and 0.6 M 1,2-dimethyl-3-*n*-propylimidazolium iodide as the electrolyte. The photocurrent/voltage characteristics were measured with a potentiostat under simulated solar light (AM 1.5, 100 mW cm^{-2}). The incident photon-to-current conversion efficiency (IPCE) spectra were recorded under monochromatic irradiation with a tungsten/halogen lamp and a monochromator. The IPCE spectra and photocurrent/voltage curves are shown in Figures 5 and 6, respectively. The IPCEs were calculated by using Equation (1).

$$\text{IPCE (\%)} = \frac{1240\ (\text{eV nm})\ J_{sc}\ (\text{mA cm}^{-2})}{\lambda\ (\text{nm})\ \Phi\ (\text{mW cm}^{-2})} \times 100 \quad (1)$$

in which J_{sc} is the short-circuit photocurrent density generated by the monochromatic light, and λ and Φ are the wavelength and intensity of the monochromatic light, respec-

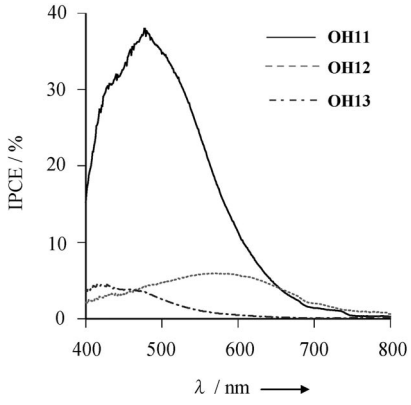

Figure 5. IPCE spectra of DSSCs based on **OH11**, **OH12** and **OH13**.

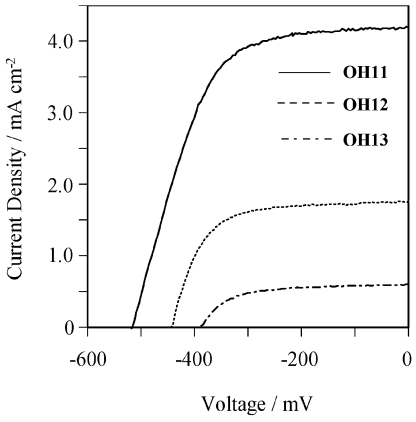

Figure 6. Photocurrent/voltage curves of the DSSCs based on **OH11**, **OH12** and **OH13**.

tively. When the performances of the DSSCs fabricated by using **OH11**, **OH12** and **OH13** as sensitizers were examined, large differences in the IPCE spectra and the photocurrent/voltage (*I*/*V*) characteristics were observed (Figures 5 and 6). The maximum IPCE value increases in the order **OH13** (4% at 470 nm) < **OH12** (6% at 600 nm) < **OH11** (38% at 500 nm). Table 4 summarizes the photovoltaic performances of DSSCs based on **OH11**, **OH12** and **OH13** as well as **OH1**, which has a carboxy group acting not only as an anchoring group for attachment to the TiO_2 surface but also as the electron acceptor. The solar energy-to-electricity conversion yield [η (%)] is expressed by Equation (2).

$$\eta\,(\%) = \frac{J_{sc}\,(\mathrm{mA\,cm^{-2}})\,V_{oc}\,(\mathrm{V})\,ff}{I_0\,(\mathrm{mW\,cm^{-2}})} \times 100 \qquad (2)$$

in which I_0 is the intensity of incident white light, V_{oc} is the open-circuit photovoltage, and *ff* represents the fill factor. Interestingly, the J_{sc} value for **OH11** (4.33 mA cm^{-2}) is similar to that for **OH1** (4.18 mA cm^{-2}) and higher than those for **OH12** (1.74 mA cm^{-2}) and **OH13** (0.62 mA cm^{-2}). The η values increase in the order **OH13** (0.15%) < **OH12** (0.51%) < **OH1** (1.24%) ≤ **OH11** (1.33%). The values of V_{oc} for **OH1**, **OH11**, **OH12** and **OH13** are 513, 525, 444 and 392 mV, respectively, which were different among the dyes.

Table 4. Photovoltaic performances of the DSSCs based on **OH1**, **OH11**, **OH12** and **OH13**.

Dye	J_{sc} [mA cm^{-2}]	V_{oc} [mV]	*ff*	η [%]
OH11	4.33	525	0.58	1.33
OH12	1.74	444	0.66	0.51
OH13	0.62	392	0.62	0.15
OH1	4.18	513	0.58	1.24

Consideration of the Relationship between Photovoltaic Performance and the Configuration of the Dye at the TiO_2 Surface

On the basis of our previous studies,[13,14] it may be safe to assume that the dye molecules lie perpendicular to the TiO_2 substrate, as shown in Figure 7. For **OH11**, the carboxy group acts as an anchoring group for attachment to the TiO_2 surface, but it cannot be the electron acceptor. From the molecular structure of **OH11**, one can assume that the pyridine ring, acting as the electron acceptor, is located in close proximity to the TiO_2 surface through the formation of a hydrogen bond between the nitrogen atom of the pyridine and a hydroxy proton at the TiO_2 surface, which is a well-known phenomenon.[15,16] Consequently, the dye **OH11** can efficiently inject electrons from the pyridine ring into the conduction band of the TiO_2 electrode through intermolecular hydrogen bonding. For **OH13**, on the other hand, the carboxy group acts as an anchoring group for attachment to the TiO_2 surface, but its ability as an electron acceptor is poor because the carboxy group is not conjugated to the dibutylamino group, which acts as the electron-donating group. Therefore, the formation of a hydrogen bond between the nitrogen atom of the pyridine and a hydroxy proton at the TiO_2 surface is difficult, in agreement with the lower electron-injection yield of **OH13** compared with **OH11**. On the other hand, the low photovoltaic performance of **OH12** is ascribable to unstable oxidized states and the relatively low LUMO level of **OH12**, which leads to a reduction in the electron-injection yield from the dye to the conduction band of TiO_2.

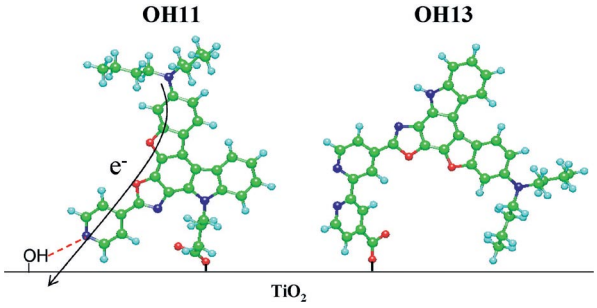

Figure 7. Plausible configurations of **OH11** and **OH13** at the TiO_2 surface. The light-blue, green, blue and red balls correspond to hydrogen, carbon, nitrogen and oxygen atoms, respectively.

Conclusions

As new-type D–π–A dye sensitizers capable of forming a strong interaction between the electron-acceptor moiety of sensitizers and the TiO_2 surface, we have designed and synthesized novel fluorescent dye **OH11** and pyridinium dye **OH12** with a pyridine and pyridinium ring as the electron-accepting group, respectively. On the basis of the molecular structure of **OH11**, it was suggested that the pyridine ring, acting as the electron acceptor, is located in close proximity to the TiO_2 surface through the formation of a hydrogen bond between the nitrogen atom of the pyridine and a hydroxy proton at the TiO_2 surface. Consequently, the dye **OH11** can efficiently inject electrons from the pyridine ring into the conduction band of a TiO_2 electrode through intermolecular hydrogen bonding. It has been concluded that a carboxy group in D–π–A dye sensitizers is necessary not as the electron acceptor, but only as an anchoring group for attachment to the TiO_2 surface. Therefore, it has been suggested that the most important criterion for developing new and efficient donor–acceptor π-conjugated sensitizers for DSSCs is the ability of the sensitizer molecule to form a strong interaction between the electron-acceptor moiety of the sensitizer and the TiO_2 surface.

Experimental Section

General: Melting points were measured with a Yanaco MP micro-melting point apparatus. IR spectra were recorded with a Perkin–Elmer Spectrum One FT-IR spectrometer by the ATR method. Absorption spectra were recorded with a Shimadzu UV-3150 spectro-

photometer and fluorescence spectra with a Hitachi F-4500 spectrophotometer. The fluorescence quantum yields (Φ) were determined with a Hamamatsu C9920-01 instrument equipped with CCD by using a calibrated integrating sphere system (λ_{ex} = 325 nm). Cyclic voltammograms (CVs) were recorded in DMF/Et_4NClO_4 (0.1 M) solution with a three-electrode system consisting of Ag/Ag^+ as the reference electrode, a Pt plate as the working electrode and a Pt wire as the counter electrode by using a Hokuto Denko HAB-151 potentiostat equipped with a functional generator. Elemental analyses were recorded with a Perkin–Elmer 2400 II CHN analyser. ^{1}H NMR spectra were recorded with a JNM-LA-400 (400 MHz) FT NMR spectrometer with tetramethylsilane (TMS) as the internal standard. Column chromatography was performed on silica gel (KANTO CHEMICAL, 60N, spherical, neutral). Mass spectral data were acquired with a JEOL double-focusing mass spectrometer SX102A equipped with a FAB inlet system.

3-(Dibutylamino)-7-(4-pyridyl)benzofuro[2,3-*c*]oxazolo[4,5-*a*]carbazole (2) and 3-(Dibutylamino)-7-(4-pyridyl)benzofuro[2,3-*c*]oxazolo[5,4-*a*]carbazole (3): A solution of **1** (0.20 g, 0.48 mmol), pyridine-4-carbaldehyde (0.052 g, 0.48 mmol) and ammonium acetate (0.75 g, 9.73 mmol) in acetic acid (50 mL) was stirred at 90 °C for 2 h. After concentrating under reduced pressure, the resulting residue was purified by chromatography on silica gel (toluene/acetic acid, 5:1) to give **2** (0.074 g, yield 31%) as an orange powder and **3** (0.031 g, yield 12%) also as an orange powder. **2**: M.p. 256–258 °C. IR (ATR): $\tilde{\nu}$ = 3061, 1624, 1602 cm^{-1}. ^{1}H NMR ([D$_6$]acetone, TMS): δ = 1.03 (t, J = 8.00 Hz, 6 H), 1.46–1.51 (m, 4 H), 1.70–1.76 (m, 4 H), 3.54 (t, J = 7.84 Hz, 4 H), 7.04 (dd, J = 1.96, 8.00 Hz, 1 H), 7.07 (d, J = 1.96 Hz, 1 H), 7.42 (t, 1 H), 7.53 (t, 1 H), 7.82 (d, J = 8.00 Hz, 1 H), 8.23 (d, J = 6.80 Hz, 2 H), 8.58 (d, J = 8.00 Hz, 1 H), 8.74 (d, J = 8.00 Hz, 1 H), 8.90 (d, J = 6.80 Hz, 2 H), 11.55 (s, 1 H, NH) ppm. MS (FAB): m/z = 503 [M]$^+$. **3**: M.p. 264–266 °C. IR (ATR): $\tilde{\nu}$ = 3095, 1602, 1559 cm^{-1}. ^{1}H NMR ([D$_6$]-DMSO, TMS): δ = 1.00 (t, J = 8.00 Hz, 6 H), 1.39–1.46 (m, 4 H), 1.60–1.67 (m, 4 H), 3.20–3.48 (m, 4 H) (overlapping peak of dissolved water in [D$_6$]DMSO), 6.96 (dd, J = 2.20, 8.00 Hz, 2 H), 7.09 (d, J = 2.20 Hz, 1 H), 7.43 (t, 1 H), 7.54 (t, 1 H), 7.73 (d, J = 8.00 Hz, 1 H), 8.20 (d, J = 5.88 Hz, 2 H), 8.48 (d, J = 8.80 Hz, 1 H), 8.66 (d, J = 8.80 Hz, 1 H), 8.93 (d, J = 5.88 Hz, 2 H), 11.55 (s, NH) ppm. MS (FAB): m/z = 503 [M]$^+$.

Ethyl [3-(Dibutylamino)-7-(4-pyridyl)benzofuro[2,3-*c*]oxazolo[4,5-*a*]carbazol-9-yl]butyrate (4): A solution of **2** (0.4 g, 0.8 mmol) in DMF was treated with sodium hydride (60%, 0.1 g, 2.5 mmol) and stirred at room temperature for 1 h. Ethyl 4-bromobutyrate (0.8 g, 4.12 mmol) was added dropwise over 20 min, and the solution was stirred at room temperature for 2 h. After concentrating under reduced pressure, the resulting residue was dissolved in CH_2Cl_2 and washed with water. The organic extract was dried with $MgSO_4$, filtered and concentrated. The residue was purified by chromatography on silica gel (CH_2Cl_2 as eluent) to give **4** (0.39 g, yield 80%) as an orange powder. M.p. 231–234 °C. IR (ATR): $\tilde{\nu}$ = 1741 cm^{-1}. ^{1}H NMR ([D$_6$]acetone, TMS): δ = 1.02 (t, 6 H), 1.11 (t, 3 H), 1.46–1.51 (m, 4 H), 1.71–1.75 (m, 4 H), 2.36–2.40 (m, 2 H), 2.50 (t, 2 H), 3.52 (t, 4 H), 3.99–4.04 (m, 2 H), 5.12 (t, 2 H), 7.05–7.09 (m, 2 H), 7.46 (t, 1 H), 7.61 (t, 1 H), 7.86 (d, J = 8.80 Hz, 1 H), 8.31 (d, J = 6.00 Hz, 2 H), 8.57 (d, J = 9.76 Hz, 1 H), 8.75 (d, J = 8.80 Hz, 1 H), 8.92 (d, J = 6.00 Hz, 2 H) ppm. MS (FAB): m/z = 616 [M]$^+$.

[3-(Dibutylamino)-7-(4-pyridyl)benzofuro[2,3-*c*]oxazolo[4,5-*a*]carbazol-9-yl]butyric Acid (OH11): A solution of **4** (0.2 g, 0.33 mmol) in ethanol (300 mL) was added dropwise to an aqueous solution of NaOH (0.06 g, 1.6 mmol, 20 mL), whilst stirring at 70 °C. After stirring at reflux for a further 12 h, the solution was acidified to pH = 4 with 2 N HCl and concentrated under reduced pressure. The residue was dissolved in CH_2Cl_2 and washed with water. The organic extract was dried with $MgSO_4$, filtered and concentrated. The resulting residue was precipitated from CH_2Cl_2/hexane to give **OH11** (0.18 g, yield 94%) as a red powder. M.p. 280–283 °C. IR (KBr): $\tilde{\nu}$ = 3048, 1711 cm^{-1}. ^{1}H NMR ([D$_6$]DMSO, TMS): δ = 0.96 (t, 6 H), 1.36–1.42 (m, 4 H), 1.57–1.63 (m, 4 H), 2.18–2.22 (m, 2 H), 2.39 (t, 2 H), 3.40 (t, 4 H), 5.01 (t, 2 H), 6.98 (dd, J = 1.96, 8.80 Hz, 1 H), 7.08 (d, J = 1.96 Hz, 1 H), 7.44 (t, 1 H), 7.59 (t, 1 H), 7.88 (d, J = 8.80 Hz, 1 H), 8.24 (d, J = 6.00 Hz, 2 H), 8.51 (d, J = 7.80 Hz, 1 H), 8.67 (d, J = 8.80 Hz, 1 H), 8.90 (d, J = 6.00 Hz, 2 H), 12.10 (s, OH) ppm. MS (FAB): m/z = 558 [M]$^+$.

4-[9-(Carboxypropyl)-3-(dibutylamino)benzofuro[2,3-*c*]oxazolo-[4,5-*a*]carbazol-7-yl]-1-butylpyridinium Iodide (OH12): A solution of **OH11** (0.09 g, 0.15 mmol) and iodobutane (100 mg) in dry acetonitrile (100 mL) was stirred at 80 °C for 72 h. After concentrating under reduced pressure, the resulting residue was precipitated from CH_2Cl_2/hexane to give **OH12** (0.074 g, yield 62%) as a dark-purple solid. M.p. 280–282 °C (decomp.). IR (ATR): $\tilde{\nu}$ = 3048, 1736 cm^{-1}. ^{1}H NMR ([D$_6$]DMSO, TMS): δ = 0.88 (t, 3 H), 0.97 (t, 6 H), 1.32–1.42 (m, 6 H), 1.65–1.75 (m, 4 H), 1.91–1.99 (m, 2 H), 2.18–2.22 (m, 2 H), 2.38 (t, 2 H), 3.44 (t, 4 H), 4.68 (t, 2 H), 5.03 (t, 2 H), 7.00 (d, J = 8.80 Hz, 1 H), 7.07 (s, 1 H), 7.46 (t, 1 H), 7.62 (t, 1 H), 7.90 (d, J = 8.80 Hz, 1 H), 8.52 (d, J = 8.80 Hz, 2 H), 8.67 (d, J = 8.80 Hz, 1 H), 8.52 (d, J = 6.80 Hz, 1 H), 9.26 (d, J = 6.80 Hz, 2 H), 12.18 (s, OH) ppm. MS (FAB): m/z = 645 [M – I]$^+$.

4′-{3-(Dibutylamino)benzofuro[2,3-*c*]oxazolo[4,5-*a*]carbazol-7-yl}-2,2′-bipyridin-4-carboxylic Acid (OH13): A solution of **1** (0.30 g, 0.72 mmol), 2,2′-bipyridin-4,4′-dicarbaldehyde (0.17 g, 0.72 mmol) and ammonium acetate (0.82 g, 10.1 mmol) in acetic acid (50 mL) was stirred at 80 °C for 5 h. After concentrating under reduced pressure, the resulting residue was purified by chromatography on silica gel (CH_2Cl_2/methanol, 20:1) to give **OH13** (0.147 g, yield 33%) as a red powder. M.p. 285–288 °C (decomp.). IR (ATR): $\tilde{\nu}$ = 1679, 1622 cm^{-1}. ^{1}H NMR ([D$_6$]DMSO, TMS): δ = 0.99 (t, 6 H), 1.37–1.45 (m, 4 H), 1.60–1.65 (m, 4 H), 3.20–3.55 (m, 4 H) (overlapping peak of dissolved water in [D$_6$]DMSO), 6.97 (dd, J = 1.96, 9.76 Hz, 1 H), 7.08 (d, J = 1.96 Hz, 1 H), 7.39 (t, 1 H), 7.51 (t, 1 H), 7.70 (d, J = 7.80 Hz, 1 H), 7.86 (s, OH), 7.95 (d, J = 6.84 Hz, 1 H), 8.24 (d, J = 7.84 Hz, 1 H), 8.49 (d, J = 7.84 Hz, 1 H), 8.63 (d, J = 9.76 Hz, 1 H), 8.90 (s, 1 H), 8.97 (d, J = 3.92 Hz, 1 H), 9.03 (d, J = 5.84 Hz, 1 H), 9.30 (s, 1 H), 12.62 (s, NH) ppm. MS (FAB): m/z = 623 [M]$^+$.

Computational Methods: Semi-empirical calculations were carried out with the WinMOPAC Ver. 3.9 professional package (Fujitsu, Chiba, Japan). Geometry optimizations in the ground state were performed by using the AM1 method.[17] All the geometries were completely optimized (keyword PRECISE) by the eigenvector-following routine (keyword EF). Experimental absorption spectra of the four compounds were compared with the absorption data determined by the semi-empirical method INDO/S (intermediate neglect of differential overlap/spectroscopic)[18] by using the SCRF Onsager model. All INDO/S calculations were performed by using single-excitation full SCF/CI (self-consistent field/configuration interaction), which includes the configuration with one electron excited from any occupied orbital to any unoccupied orbital; 225 configurations were considered [keyword CI (15 15)].

Preparation of the Dye-Sensitized Solar Cells Based on Dyes OH1, OH11, OH12 and OH13: The TiO_2 paste (JGC Catalysts and Chemicals Ltd., PST-18NR) was deposited on a fluorine-doped tin oxide (FTO) substrate by doctor-blading and sintered at 450 °C for

50 min. The 9 μm thick TiO_2 electrode (photoactive area 0.5 × 0.5 cm) was immersed in a 0.1 mM tetrahydrofuran solution of the dye for a sufficient number of hours to adsorb the photosensitizer. The DSSCs were fabricated by using the TiO_2 electrode thus prepared, Pt-coated glass as the counter electrode and a solution of 0.05 M iodine, 0.1 M lithium iodide and 0.6 M 1,2-dimethyl-3-*n*-propylimidazolium iodide in acetonitrile as the electrolyte. The photocurrent/voltage characteristics were measured under simulated solar light (AM 1.5, 100 mW cm^{-2}) by using a potentiostat. IPCE spectra were recorded under monochromatic irradiation with a tungsten/halogen lamp and a monochromator. The absorption spectra of the dye-adsorbed TiO_2 films were recorded in the diffuse-reflection mode by using a JASCO UV/Vis spectrophotometer with a calibrated ISV-469 integrating sphere system.

Acknowledgments

This work was supported by Grants-in-Aid for Scientific Research (B) (19350094) from the Ministry of Education, Science, Sports and Culture of Japan and by the Nissan Science Foundation.

[1] a) B. O'Regan, M. Grätzel, *Nature* **1991**, *353*, 737–740; b) A. Hagfeldt, M. Grätzel, *Chem. Rev.* **1995**, *95*, 49–68; c) U. Bach, D. Lupo, P. Comte, J. E. Moser, F. Weissörtel, J. Salbeck, H. Spreitzer, M. Grätzel, *Nature* **1998**, *395*, 583–585; d) M. Grätzel, *Nature* **2001**, *414*, 338–344; e) N. Robertson, *Angew. Chem. Int. Ed.* **2006**, *45*, 2338–2345; f) P. Xie, F. Guo, *Curr. Org. Chem.* **2007**, *11*, 1272–1286; g) N. Robertson, *Angew. Chem. Int. Ed.* **2008**, *47*, 1012–1014.

[2] Y. Ooyama, Y. Kagawa, Y. Harima, *Eur. J. Org. Chem.* **2009**, 2903–2934.

[3] Z. Chen, F. Li, C. Huang, *Curr. Org. Chem.* **2007**, *11*, 1241–1258.

[4] a) Z.-S. Wang, Y. Cui, K. Hara, Y. Dan-oh, C. Kasada, A. Shinpo, *Adv. Mater.* **2007**, *19*, 1138–1141; b) Z.-S. Wang, Y. Cui, Y. Dan-oh, C. Kasada, A. Shinpo, K. Hara, *J. Phys. Chem. C* **2008**, *112*, 17011–17017.

[5] a) I. Jung, J. K. Lee, K. H. Song, K. Song, S. O. Kang, J. Ko, *J. Org. Chem.* **2007**, *72*, 3652–3658; b) D. P. Hagberg, J.-H. Yum, H. Lee, F. D. Angelis, T. Marinado, K. M. Karlsson, R. Humphry-Baker, L. Sun, A. Hagfeldt, M. Grätzel, M. K. Nazeeruddin, *J. Am. Chem. Soc.* **2008**, *130*, 6259–6266; c) K. R. J. Thomas, J. T. Lin, Y.-C. Hsu, K.-C. Ho, *Chem. Commun.* **2008**, 4098–4100; d) G. Zhou, N. Pschirer, J. C. Schöneboom, F. Eickemeyer, M. Baumgarten, K. Müllen, *Chem. Mater.* **2008**, *20*, 1808–1815; e) W. Xu, B. Peng, J. Chen, M. Liang, F. Cai, *J. Phys. Chem. C* **2008**, *112*, 874–880; f) Z. Ning, Q. Zhang, W. Wu, H. Pei, B. Liu, H. Tian, *J. Org. Chem.* **2008**, *73*, 3791–3797; g) G. Li, K.-J. Jiang, Y.-F. Li, S.-L. Li, L.-M. Yang, *J. Phys. Chem. C* **2008**, *112*, 11591–11599.

[6] a) Z.-S. Wang, F.-Y. Li, C.-H. Huang, L. Wang, M. Wei, L.-P. Jin, N.-Q. Li, *J. Phys. Chem. B* **2000**, *104*, 9676–9682; b) Y.-S. Chen, C. Li, Z.-H. Zeng, W.-B. Wang, X.-S. Wang, B.-W. Zhang, *J. Mater. Chem.* **2005**, *15*, 1654–1661.

[7] a) N. Koumura, Z.-S. Wang, S. Mori, M. Miyashita, E. Suzuki, K. Hara, *J. Am. Chem. Soc.* **2006**, *128*, 14256–14257; b) S. Kim, J. K. Lee, S. O. Kang, J. Ko, J.-H. Yum, S. Frantacci, F. D. Angelis, D. D. Censo, M. K. Nazeeruddin, M. Grätzel, *J. Am. Chem. Soc.* **2006**, *128*, 16701–16707; c) Z.-S. Wang, N. Koumura, Y. Cui, M. Takahashi, H. Sekiguchi, A. Mori, T. Kubo, A. Furube, K. Hara, *Chem. Mater.* **2008**, *20*, 3993–4003; d) H. Choi, C. Baik, S. O. Kang, J. Ko, M.-S. Kang, M. K. Nazeeruddin, M. Grätzel, *Angew. Chem. Int. Ed.* **2008**, *47*, 327–330; e) H. Qin, S. Wenger, M. Xu, F. Gao, X. Jing, P. Wang, S. M. Zakeeruddin, M. Grätzel, *J. Am. Chem. Soc.* **2008**, *130*, 9202–9203.

[8] a) T. Horiuchi, H. Miura, S. Uchida, *Chem. Commun.* **2003**, 3036–3037; b) T. Horiuchi, H. Miura, S. Uchida, *J. Photochem. Photobiol. A: Chem.* **2004**, *164*, 29–32; c) T. Horiuchi, H. Miura, K. Sumioka, S. Uchida, *J. Am. Chem. Soc.* **2004**, *126*, 12218–12219; d) L. Schmidt-Mende, U. Bach, R. Humphry-Baker, T. Horiuchi, H. Miura, S. Ito, S. Uchida, M. Grätzel, *Adv. Mater.* **2005**, *17*, 813–815; e) S. Ito, S. M. Zakeeruddin, R. Humphry-Baker, P. Liska, R. Charvet, P. Comte, M. K. Nazeeruddin, P. Péchy, M. Takata, H. Miura, S. Uchida, M. Grätzel, *Adv. Mater.* **2006**, *18*, 1202–1205; f) W. H. Howie, F. Claeyssens, H. Miura, L. M. Peter, *J. Am. Chem. Soc.* **2008**, *130*, 1367–1375; g) D. Kuang, S. Uchida, R. Humphry-Baker, S. K. Zakeeruddin, M. Grätzel, *Angew. Chem. Int. Ed.* **2008**, *47*, 1923–1927; h) S. Ito, H. Miura, S. Uchida, M. Takata, K. Sumioka, P. Liska, P. Comte, P. Péchy, M. Grätzel, *Chem. Commun.* **2008**, 5194–5196.

[9] a) T. Edvinsson, C. Li, N. Pschirer, J. Schöneboom, F. Eickemeyer, R. Sens, G. Boschloo, A. Herrmann, K. Müllen, A. Hagfeldt, *J. Phys. Chem. C* **2007**, *111*, 15137–15140; b) Y. Shibano, T. Umeyama, Y. Matano, H. Imahori, *Org. Lett.* **2007**, *9*, 1971–1974; c) T. Edvinsson, C. Li, N. Pschirer, J. Schöneboom, F. Eickemeyer, R. Sens, G. Boschloo, A. Herrmann, K. Müllen, A. Hagfeldt, *J. Phys. Chem. C* **2007**, *111*, 15137–15140.

[10] a) J. Rochford, D. Chu, A. Hagfeldt, E. Galoppini, *J. Am. Chem. Soc.* **2007**, *129*, 4655–4665; b) A. Forneli, M. Olanells, M. A. Sarmentero, E. Matyinez-Ferrero, B. C. O'Regan, P. Ballester, E. Palomares, *J. Mater. Chem.* **2008**, *18*, 1652–1658; c) S. Eu, S. Hayashi, T. Umeyama, Y. Matano, Y. Araki, H. Imahori, *J. Phys. Chem. C* **2008**, *112*, 4396–4405; d) S. Hayashi, Y. Matsubara, S. Eu, H. Hayashi, T. Umeyama, Y. Matano, H. Imahori, *Chem. Lett.* **2008**, *37*, 846–847.

[11] a) Y. Chen, Z. Zeng, C. Li, W. Wang, X. Wang, B. Zhang, *New J. Chem.* **2005**, *29*, 773–776; b) S. Tatay, S. A. Haque, B. O'Regan, J. R. Durrant, W. J. H. Verhees, J. M. Kroon, A. Vidal-Ferran, P. Gaviña, E. Palomares, *J. Mater. Chem.* **2007**, *17*, 3037–3044; c) J.-H. Yum, P. Walter, S. Huber, S. Rentsch, T. Geiger, F. Nüesch, F. D. Angelis, M. Grätzel, M. K. Nazeeruddin, *J. Am. Chem. Soc.* **2007**, *129*, 10320–10321; d) A. Burke, L. Schmidt-Mende, S. Ito, M. Grätzel, *Chem. Commun.* **2007**, 234–236; e) A. Burke, S. Ito, H. Snaith, U. Bach, J. Kwiatkowski, M. Grätzel, *Nano Lett.* **2008**, *8*, 977–981.

[12] a) E. Palomares, M. V. Martinez-Diaz, S. A. Haque, T. Torres, J. R. Durrant, *Chem. Commun.* **2004**, 2112–2113; b) A. Morandeira, I. López-Duarte, M. V. Martinez-Diaz, B. O'Regan, C. Shuttle, N. A. Haji-Zainulabidin, T. Torres, E. Palomares, J. R. Durrant, *J. Am. Chem. Soc.* **2007**, *129*, 9250–9251; c) P. Y. Reddy, L. Giribabu, C. Lyness, H. J. Snaith, C. Vijaykumar, M. Chandrasekharam, M. Lakshmikantam, J.-H. Yum, K. Kalyanasundaram, M. Grätzel, M. K. Nazeeruddin, *Angew. Chem. Int. Ed.* **2007**, *46*, 373–376; d) J.-J. Cid, J.-H. Yum, S.-R. Jang, M. K. Nazeeruddin, E. Martinez-Ferrero, E. Palomares, J. Ko, M. Grätzel, T. Torres, *Angew. Chem. Int. Ed.* **2007**, *46*, 8358–8362; e) B. C. O'Regan, I. López-Duarte, M. V. Martinez-Diaz, A. Forneli, J. Albero, A. Morandeira, E. Palomares, T. Torres, J. R. Durrant, *J. Am. Chem. Soc.* **2008**, *130*, 2906–29071; f) S. Eu, T. Katoh, T. Umeyama, Y. Matano, H. Imahori, *Dalton Trans.* **2008**, 5476–5483.

[13] a) Y. Ooyama, Y. Harima, *Chem. Lett.* **2006**, *8*, 902–903; b) Y. Ooyama, Y. Kagawa, Y. Harima, *Eur. J. Org. Chem.* **2007**, 3613–3621; c) Y. Ooyama, A. Ishii, Y. Kagawa, I. Imae, Y. Harima, *New J. Chem.* **2007**, *31*, 2076–2082; d) Y. Ooyama, Y. Shimada, Y. Kagawa, I. Imae, Y. Harima, *Org. Biomol. Chem.* **2007**, *5*, 2046–2054.

[14] a) Y. Ooyama, Y. Shimada, Y. Kagawa, Y. Yamada, I. Imae, K. Komaguchi, Y. Harima, *Tetrahedron Lett.* **2007**, *48*, 9167–9170; b) Y. Ooyama, Y. Shimada, A. Ishii, G. Ito, Yu. Kagawa, I. Imae, K. Komaguchi, Y. Harima, *J. Photochem. Photobiol. A: Chem.* **2009**, *203*, 177–185.

[15] a) H.-P. Boehm, H. Knözinger in *Catal.*: *Sci. Technol.* (Eds.: J. R. Anderson, M. Boudart), Springer, Berlin, **1983**, vol. 4, pp.

40–189; b) N. Sheppard in *Vibrational Spectroscopy of Adsorbates* (Ed.: R. F. Willis), Springer, Berlin, **1980**, pp. 165–176; c) J. B. Peri in *Catal.: Sci. Technol.* (Eds.: J. R. Anderson, M. Boudart), Springer, Berlin, **1984**, vol. 5, pp. 171–220; d) A. A. Davydov in *Infrared Spectroscopy of Adsorbed Species on the Surface of Transition Metal Oxide* (Ed.: C. H. Rochester), Wiley, Chichester, **1984**; e) A. T. Bell, "Methods of Surface Characterization" in *Vibrational Spectroscopy of Molecules on Surfaces* (Eds.: J. T. Yates Jr, T. E. Madey), Plenum Press, New York, **1987**, vol. 1, pp. 105–133; f) M. W. Urban, *Vibrational Spectroscopy of Molecules and Macromolecules on Surfaces*, Wiley, Chichester, **1993**, pp. 171–185.

[16] a) M. I. Zaki, M. A. Hasan, F. A. Al-Sagheer, L. Pasupulety, *Colloids Surf. A* **2001**, *190*, 261–274; b) T. J. Dines, L. D. MacGregor, C. H. Rochester, *Spectrochim. Acta Part A* **2003**, *59*, 3205–3217; c) M. Akcay, *Appl. Catal. A* **2005**, *294*, 156–160; d) S. M. Andonova, G. S. Şentürk, E. Kayhan, E. Ozensoy, *J. Phys. Chem. C* **2009**, *113*, 11014–11026.

[17] M. J. S. Dewar, E. G. Zoebisch, E. F. Healy, J. J. Stewart, *J. Am. Chem. Soc.* **1985**, *107*, 3902–3909.

[18] a) J. E. Ridley, M. C. Zerner, *Theor. Chim. Acta* **1973**, *32*, 111–134; b) J. E. Ridley, M. C. Zerner, *Theor. Chim. Acta* **1976**, *42*, 223–236; c) A. D. Bacon, M. C. Zerner, *Theor. Chim. Acta* **1979**, *53*, 21–54; d) H. A. Kurtz, J. J. P. Stewart, D. M. Dieter, *J. Comput. Chem.* **1990**, *11*, 82–87.

Received: August 28, 2009
Published Online: November 24, 2009

